Bull. Spec. Astrophys. Obs., 1996, 41, 64–79

Multi–frequency observations of supernova remnants with the RATAN–600 radio telescope

S. A. Trushkin

Special Astrophysical Observatory of the Russian AS, Nizhnij Arkhyz 357147, Russia

Abstract.
The results of multi–frequency observations of about 90 Galactic supernova remnants (SNR) in the Galactic quadrants I and IV at 2–6 frequencies are presented. The main goals are to determine accurately sizes, structure and radio spectra. The observations were carried out with the Northern sector of the RATAN–600 radio telescope at 0.96, 2.3, 3.65, 3.9, 7.7 and 11.2 GHz in 1987–1995. Flux densities of the most SNRs have been measured at 0.96 and 3.9 GHz. The new suspected SNRs were included in the recent runs of observations (1992–1996). The spectra of many new SNRs have been defined with a higher accuracy. The one–dimensional brightness distributions of all SNRs have been analyzed comparing with the available radio maps. The interesting variable point source 1820–239 was identified with the confirmed SNR G8.7–5.0. It has a non–thermal spectrum and shows flux variability on a time scale of 3–4 months. In the confused region G10.3–0.3 we have clearly found a non–thermal detail in the new observations. G12.0–0.1 resolved into two sources: W–detail has a flat spectrum and E–detail has a steep one. Suspected G36.6–0.7 has the spectral index -0.8, it seems to be a background extragalactic source because the spectral index is too steep for SNR. For 18 SNRs (G5.9+3.1, G8.7–5.0, G11.2–1.2, G13.5+0.2, G16.7+0.1, G16.8–1.1, G17.4–2.3, G23.6+0.3, G42.8+0.6, G45.9+1.6, G49.2–0.7, G57.2+0.8, G59.5+0.1, G59.8+1.8, G68.6–1.2, G344.7–0.1, G348.5–0.0 and G352.7–0.1) the non–thermal spectra ($\alpha < -0.3$) have been confirmed. Another 16 shell SNRs (G0.9+0.1, G1.4–0.1, G4.2–3.5, G5.2–2.6, G5.4–1.2, G6.4+4.0, G15.1+1.6, G17.8–2.6, G32.8–0.1, G40.5–0.5, G43.9+1.6, G73.9+0.9, G85.2–1.2, G351.2+0.1, G357.7+0.3, G359.1–0.5 have a flatter, critical spectral index $\alpha > -0.3$ as it follows from our flux points. The new spectra of 12 SNRs have strongly changed ($\Delta\alpha > 0.1$). In the region of the SNR G5.4–1.2 the compact source G5.27–0.90, associated with the pulsar PSR 1758–24, has shown the inverse spectrum with the spectral index $\alpha = +0.33$, which is consistent with the optically thin synchrotron source with a mono–energetic spectrum of relativistic electrons. Unusual SNR G18.9–1.1 has a prominent feature with a flat spectrum, and the rest of the remnant has a steep one. The central W–E "plateau" within the remarkable SNR CTB80 has the spectral index $\alpha = -0.52 \pm 0.06$. But the $40'' \times 30''$ "core" near the 40 ms pulsar from 1 to 15 GHz has shown a flat spectrum, at the level of 1.0 Jy, and during the last six years this level has not changed. However a turnover at high frequencies is possible. There are no variations of the spectral index from the brighter W–region to the weak E–part of the G357.7–0.1, rejecting possible speculations about "aging" of radio emission within the remnant from the bright filamentary region to the faint smoothed one. During the last years the RATAN–600 has been used to carry out a new survey of the Galactic plane at 960 and 3900 MHz from $l = 342°$ to $l = 19°$, $|b| < 5.5°$, to search for new SNRs and to study the SNRs that have just been detected.

Key words: supernova remnants – galactic radio sources – radio continuum

1. Introduction

The remnants of supernova outbursts are the key objects in stellar astrophysics, problem of black holes and neutron stars origin, energetics of Galactic cosmic rays and formation of the total structure of interstellar medium.

Galactic supernova (SN) outbursts themselves very rare phenomena near the Sun and in the Galaxy they occur about 2–3 times a century. But cause of the strong interstellar absorption such ev are not detected in the optical range. The SN 19 in the Large Magellanic Cloud is the only bright

pernova, observed with the naked eye ($V_{max} = 4^m$) for the last 400 years, since the time Kepler observed his SN in our Galaxy. Therefore the data about such events in the Milky Way were collected indirectly, using observations of the hot expanded gas envelopes of SN ejecta, named supernova remnants. Optical emission of gas in these envelopes shows that it is heated from 10000 up to 10 millions K, and the last value corresponds to the X–ray emission of the gas behind the shock wave front. Arendt (1989) has analyzed IRAS data and showed that dust formed in a SN explosion, and interstellar dust swept by envelope of SNR are sources of prominent IR radiation, while SNRs have not any special IR characteristics.

At last, in the radio wave range all SNRs emit intensive non–thermal synchrotron radiation, arising from electrons moving in a magnetic field with a velocity close to that of light. These electrons could be born at the earliest time of expansion of SN envelope, could be continuously injected by pulsars into plerionic SNRs, or heap up and re–accelerate at the later stages of SNR evolution in ISM. These variants result in a variety of forms of radio SNRs. Shells and plerions have different radio structures, old SNRs differ from young ones in brightness and structure. Samples of Galactic SNRs (detected in radio $\approx$ 190, in IR $\approx$ 50, in optics $\approx$ 70, in X–rays $\approx$ 60) are collected in the catalogs by Green (1995), Arendt (1989), van den Bergh (1983) and Seward (1990).

Even simple evaluations show their incompleteness both in minimum flux and in surface brightness and angular sizes. The most sensitive surveys in the region $|b| < 10^o$ could increase the number of SNRs 2–3 times. In 1989 the author carried out a SNR search among unidentified extended radio sources (Trushkin, 1989b, 1991b), and some new SNR candidates were detected.

It should be noted that the problem of search for SNRs must not be restricted only to the search for extended sources with non–thermal spectrum. It is necessary to analyze the most probable places of SN bursts, star–formation regions and OB–associations, and to separate the thermal and non–thermal sources.

The problem of confusion SNRs with HII regions can be resolved by using the IRAS data (catalogs and maps) and measuring linear polarization of radio emission from these regions. Multi–frequency radio observations allowed revealing of spectral peculiarities of radio emission of the SNRs.

The author has used the electronic version of IRAS point source catalog (IPSC) (Beichman et al., 1988) and made the selection programs for it. We have made a modification of IPSC electronic version, adapted for data–base use (Verkhodanov and Trushkin, 1994). Hughes and McLeod (1989) have used the special criteria in order to indicate the thermal sources separating all HII regions and planetary nebulae (PN) from IPSC. This work was repeated and the whole catalog consists of 2295 HII regions and 995 PNs in the region $|b| < 10^o$. The IR–sources in the areas of SNRs were also selected as in the paper of Arendt (1989).

In organizing investigation of Galactic SNRs one must take into account the following facts.

- Good sensitive surveys in the Galactic plane have been carried out at the centimeter wavelengths with the arcmin resolution with the Effelsberg 100 m (Reich et al., 1990a) and the Nabeyama 45 m telescopes (Handa et al., 1987). Thus, measurements of intensity and polarization in the wider wavelength range should be continued in these regions.

- Some SNRs were observed by American researchers with the large VLA interferometer for obtaining very high resolution radio maps. A comparison of the brightness distributions of these SNRs and our one–dimensional drift scans is possible in order to detect spectral details of synchrotron radiation, using the multi–frequency ability of the RATAN–600. For the Crab nebula such comparison has been made by the author (Trushkin, 1986).

- On the other hand the southern part of the Galaxy was studied only with Australian telescopes, having moderate sensitivity and resolution. The region of the Galactic quadrants I and IV has the longest way in the Galactic disk, because it is directed to the Center of the Galaxy. Thus this region seems to be the most interesting for search for SNRs. There are 20–25 known SNRs, but no good radio maps are available for them. Only recently the data of the MOST survey became accessible (Gray, 1994; Whiteoak and Green, 1996). All SNRs in the second Galactic quadrant were investigated in the earlier paper by Trushkin et al. (1988). A few of the new results were presented in the thesis (Trushkin, 1989).

2. Observations

We compiled a list of the observed SNRs from the catalogs of Green (1991, 1995). We also used the data from Kovalenko et al. (1994a, 1994b). First of all we took the SNRs with the angular diameter $D < 30'$ and the ones with a sparse number of radio data. In the observational runs of 1991–1992 the complex regions in the Galactic quadrants I and IV were investigated, where there were many known SNRs. Almost all of them were observed. Also in the first part of the new Galactic survey, $342^o < l < 360^o$ and $|b| < 5.5^o$, in 1991-1992 (hereafter — ZG–survey, Trushkin, 1994, 1996) the "neutral area" of the Galaxy $|b| > 3^o$ was included. In this region, $2^o < |b| < 5^o$, many new SNRs were found.

Table 1: *RATAN-600 observed and derived parameters of SNRs*

Name $lll.l \pm b.b$ (1)	RA50 hh mm ss (2)	Dec50 dd mm (3)	Size arcmin (4)	S_ν 2.7cm (5)	S_ν 7.6cm (6)	S_ν 13 cm (7)	(Jy) 1GHz (8)	Sp. old (9)	Ind. new (10)
0.9 +0.1	17 44 12	−28 08	8(6.6)		9.3		/18?	var	0.26
1.4 −0.1	17 46 30	−27 45	10		2.5		/2?	?	0.0
1.9 +0.3	17 45 37	−27 09	1.2	0.15	0.45		/0.6	0.7	0.62
4.2 −3.5	18 05 45	−27 04	(28)		2.45		4.7/3.2?	0.6?	0.2
4.5 +6.8	17 27 43	−21 27	3		8.3	12.3	21/19.	0.64	0.63
5.2 −2.6	18 04 25	−25 45	(18)		1.1		1.6/2.6	0.6?	0.2
5.4 −1.2	17 59 00	−24 50	35		21.0	23.0	33/35.	0.2?	0.2
5.9 +3.1	17 44 20	−22 15	20		1.3		4.0/3.3?	0.4	0.36
6.1 +1.2	17 51 55	−23 05	30×26		1.45		4.8/4.0	0.3?	0.8
6.1 −0.1	17 57 30	−23 25	42		170		300/310	var	
6.4 +4.0	17 42 10	−21 20	31		1.2		1.8/1.3?	0.4?	0.2
7.7 −3.7	18 14 20	−24 05	18(21)		6.7		11.8/10	0.32	0.35
8.7 −5.0	18 21 05	−23 50	(26)25.4		4.4		8.9/4.4	0.3	0.50
8.7 −0.1	18 02 35	−21 25	(45)		63.0		95/90	0.25	0.28
9.8 +0.6	18 02 10	−20 14	12		1.9		4.1/3.9	0.5	0.52
10.0 −0.3	18 05 40	−20 26	8?(5.7)	0.37	0.45	0.94	- /2.9	0.8	0.7
11.2 −0.3	18 08 30	−19 26	4 (4.7)		9.5		17/22	0.49	0.46
11.2 −1.2	18 11 10	−19 48	17×14		5.0	7.0	9.0/		0.40
11.4 −0.1	18 07 50	−19 06	8		1.7		/6	0.5	0.50
12.0 −0.1	18 09 15	−18 38	5?(2.4)E	0.15	0.4		2.6/3.5	0.7	1.0
	18 08 55	−18 38	(1.)W	1.73	2.3				0.12
13.5 +0.2	18 11 20	−17 13	5×4	0.46	0.7	2.0	-/3.5?	1.0?	0.5
15.1 −1.6	18 21 05	−16 36	30×24(30)		3.9		4.8/5.5?	0.8?	0.2
15.9 +0.2	18 16 00	−15 03	7×5(5.1)	1.05	1.9		4.0/4.5	0.7?	0.62
16.7 +0.1	18 18 07	−14 22	3	1.05	2.1		4.8/3.5	0.7	0.33
16.8 −1.1	18 22 30	−14 48	30×24?	3.0	7.0		15/2?	?	0.37
17.4 −2.3	18 28 05	−14 54	24?(22)		2.0		5.4/4.8?	0.8?	0.46
17.8 −2.6	18 30 00	−14 41	24?(25)		2.1		2.2/4.0?	0.3?	0.20
18.8 +0.3	18 21 10	−12 25	18×13(15)		18.9		28 /27	0.4	0.40
18.9 −1.1	18 27 00	−13 00	33(33.5)		18.9		34/37	var	0.34
20.0 −0.2	18 25 20	−11 37	10(11)		7.1		6.9/10	0.0	0.04
21.5 −0.9	18 30 37	−10 37	1.2(1)	6.25	6.4	6.0	5/6	0.0	0.0
21.8 −0.6	18 30 00	−10 10	20(21)		28.0		63/69	0.5	0.61
22.7 −0.2	18 30 00	−09 15	25(part)				60/69	0.5	0.61
23.6 +0.3	18 30 20	−08 15	10?(13)		3.3	4.6	7.2/8?	0.3	0.51
24.7 +0.6	18 31 30	−07 07	30×15(20)		7.0	7.0	6.5/20?	0.2	0.0
24.7 −0.6	18 36 00	−07 35	15?(17)		2.6		7.5/8	0.5	0.72
27.4 +0.0	18 38 40	−04 59	4(4.8)		1.65		4.0/6	0.68	0.71
27.8 +0.6	18 37 06	−04 28	50×35(40)		20.0	25.4	32.6/30	var	0.52
29.7 −0.3	18 43 48	−03 02	3(3.7)	1.6	3.9		9.8/10	0.7	0.60
30.7 −2.0	18 51 50	−02 58	16		0.45		1.5/0.5	0.7	0.6
30.7 +1.0	18 42 10	−01 35	24×18(18)		2.84		5.8/6	0.4	0.34
31.9 +0.0	18 46 50	−00 59	5(7.1)	5.6	11.3		26./24	0.55	0.50
32.8 −0.1	18 48 50	−01 12	17(13)		5.5		5.6/11?	0.2?	0.00
33.6 +0.1	18 50 15	+00 37	10(10)	6.5	8.5		15 /22	0.5	0.60
34.7 −0.4	18 53 30	+01 18	35× 27		136	190	306/230	0.30	0.37

Table 1: (continued)

(1)	(2)	(3)	(4)	(5)	(6)	(7)	(8)	(9)	(10)
36.6 +2.6	18 46 20	+04 23	17×13?		0.65	0.76	0.81/0.7?	0.5?	0.11
36.6 −0.7	18 58 05	+02 52	25(25)		3.0		11.5/?	0.6?	0.8
39.2 −0.3	19 01 40	+05 23	11×6(11)		11.5	13.4	21/18	0.6	0.42
39.7 −2.0	19 10 00	+04 50	120×60		32	44	65/85?	0.7?	0.49
40.5 −0.5	19 04 45	+06 26	22(21)		8.6		10./11	0.5	0.10
41.1 −0.3	19 05 08	+07 03	4.5×2.5	2.66	6.7		8.5/22	0.48	0.71
42.8 +0.6	19 04 55	+09 00	24(24)		1.44		4.7/3?	0.5?	0.72
43.3 −0.2	19 08 44	+09 01	4×3(4.3)	10.4	18.8		37/38	0.48	0.50
43.9 +1.6	19 04 30	+10 25	(12)E-part		1.0		1.0/8.6?	0.0?	0.0
43.9 +1.6	19 03 00	+10 50	(10)N-part		0.9		3.5/	0.0?	1.00
45.7 −0.4	19 14 05	+11 04	22(21)	1.5	4.0		12.6/4.2	0.4?	0.63
46.8 −0.3	19 15 50	+12 04	17×13(18)	5.3	9.0		15.8/14	0.42	0.57
49.2 −0.7	19 21 30	+14 00	25?part	33	124		174/160?	0.3?	0.65
53.6 −2.2	19 36 30	+17 08	28(32)		4.1		10.8/8	0.6	0.58
54.1 +0.3	19 28 28	+18 46	1.5	0.43	0.45		0.4/0.5	0.1	0.06
55.7 +3.4	19 19 10	+21 38	23		0.75		/1.4	0.6	0.3
57.2 +0.8	19 32 50	+21 50	12?(7.9)		0.8	0.9	1.8/1.8	?	0.41
59.5 +0.1	19 40 25	+23 28	5		1.4	1.75	2.7/3?	?	0.57
59.8 +1.2	19 36 50	+24 12	20×16(11)		0.8		1.50/1.6	0.5?	0.36
65.7 +1.2	19 50 10	+29 18	18(15.8)		2.05		5.7/5.1	0.6	0.63
67.7 +1.8	19 52 34	+31 21	9(10.5)		0.6	1.05	2.2/1.4	0.3	0.64
68.6 −1.2	20 06 40	+30 28	28×25?		0.26		/0.7?	0.0?	0.5
69.7 +1.0	20 00 45	+32 35	16		1.3		3.0/1.6	0.8	0.6
73.9 +0.9	20 12 20	+36 03	22?(25)		5.2		8.9/9	0.3?	0.20
74.9 +1.2	20 14 10	+37 03	8x6(10)	2.6	6.0		9/9	var	.2-.8
78.2 +2.1	20 19 00	+40 15	60		150	186	323/340	0.6	0.53
83.0 −0.2	20 44 07	+42 42	10		0.95	1.25	1.0/0.8	-	0.0
84.2 −0.8	20 51 30	+43 16	20×16		3.5	5.5	10.5/11	0.5	0.62
84.9 +0.5	20 48 45	+44 42	6(10)	1.3	2.0	2.8	6.0/0.8	-	0.60
85.2 −1.2	20 57 12	+43 45	6		1.7	1.4	2.3/	0.7	0.03
327.6 +14.	14 59 35	−41 44	30		9.2	13.0	/19	0.6	0.53
344.7 −0.1	17 00 20	−41 38	8?(8.3)		1.4	1.65	3.6/3.5	0.4?	0.53
346.6 −0.2	17 06 50	−40 07	8(10.2)	2.9	6.3	8.8	11.4/10	0.5	0.45
348.5 +0.1	17 10 40	−38 29	10(10.8)		41		118 /72	0.3	0.46
348.7 +0.3	17 10 30	−38 08	10(8)		21		/26	0.3	0.29
349.7 +0.2	17 14 35	−37 23	2.5×2	4.0	8-11	15.5	25/20	0.5	0.42
350.0 −1.8	17 23 40	−38 20	30(44)		9.2		15/31	0.5	0.50
350.1 −0.3	17 17 40	−37 24	4?(6.4)		2.1	3.2	6.2/5.6	0.7	0.84
351.2 +0.1	17 19 05	−36 08	6×4(6.5)	2.7	2.6	3.9	3.3/5.8	0.4	0.24
352.7 −0.1	17 24 20	−35 05	6×5(6.3)	1.4	2.6		/6?	0.6?	0.58
355.9 −2.5	17 42 35	−33 42	13(15)		4.0		7.6/8	0.5	0.50
357.7 −0.1	17 37 15	−30 56	12×6(16)	8.6	22		43/37	0.4	0.48
357.7 +0.5	17 35 20	−30 42	24(27)		6.1		7.2/10	0.4?	0.15
359.1 −0.5	17 42 20	−29 56	24(29)		15.5		/14	0.4?	0.0?

Column (1) lists Galactic notation names of the new and well–known SNRs from Green's catalog; columns (2) and (3) give Right Ascension and Declination (epoch 1950.0), column (4) contains angular sizes of a source: MAX×MIN and the new measured size in parentheses, if it is different; columns (5), (6), (7) present measured flux densities (S_ν) at 2.7, 7.6 and 13 cm wavelengths; column (8) contains S_ν at 960 MHz and estimated values at 1 GHz from Green's catalog; in column (9) the "old" spectral indices from Green's Table 1 and in column (10) the "new" ones (here $S \sim \nu^{-\alpha}$) evaluated from the available and measured points S_ν are given. The sign "?" means sparse data or great uncertainty. The sign "var" means variable over remnants.

The observations were carried out in meridian transit of the Galactic plane through the immovable beam pattern of the antenna ("Northern sector") of the RATAN–600 radio telescope. Observations were conducted with a complex of continuum wide–band radiometers. Measurements of flux densities of almost all SNRs at 0.96 and 3.9 GHz were made, additional flux points, however, were obtained at 2.3, 7.7 and 11.2 GHz.

The realized sensitivity is equal to 50, 40, 15, 40 100 mJy at 0.96, 2.3, 3.9, 7.7 and 11.2 GHz, respectively, which is higher than the accuracy of determination of zero level of extended SNRs against the complex Galactic background. It corresponds to 40 and 5 mJy/beam of brightness temperature sensitivity at 0.96 and 3.9 MHz. In our early observations we used the 3.65 GHz radiometer with a parametric amplifier. The 3.9, 7.7 and 11.2 GHz radiometers have the HEMT preamplifiers cooled with a closed cryogenic system down to 12 K. The 960 MHz radiometer is based on the low–noise, non–cooled and wide–band transistor amplifier. In the last observation run a new radiometer at 11 GHz was added with a noise level of about 20 mJy/beam, where the beam is $25'' \times 14'$. This radiometer is also cooled by a closed cryogenic system. The resolution (HPBW, RA×Dec) is $4' \times 75'$ and $1' \times 39'$ at 0.96 and 3.9 GHz, respectively in observations of the southern SNRs. The resolution for the region of declination 20 — 45 is $3' \times 16'$ and $1' \times 4'$ at the same frequencies. The calibration of day–to–day changes in gain and pointing was provided by observations of the sources 3C48, PKS 0237-23, 3C161, PKS 1245-19, 3C286, NGC 7027 and DR21 and some sources from the list of Aliakberov et al. (1985), for which the flux densities were accepted in accordance with Baars (1977) scale. Each observation was repeated 3–5 times in order to minimize atmospheric fluctuations. The total errors of measurements of flux densities are equal to 5–15%.

A new system *prat* of data processing of the obtained f–files (type of FITS–files), adapted for galactic scans and extended sources, was made for MS DOS. A program was compiled in MS 7.00 with the standard libraries. This interactive program, based on the old packages for the minicomputer SM1420 by Vitkovskij (1990), was created by Sokolova and Trushkin in 1991–92. Now it consists of new procedures of subtracting the Galactic background, based on spline approximations, antenna temperature/flux density calibrations and cleaning from interferences by means of Hodges–Lehmann smoothing (Verkhodanov et al., 1988). Here all the figures of drift scans are obtained with *prat*. In Table 1 we have included the flux density measurements of new SNRs and ones from the Green's catalogs of SNRs (1988; 1991; 1995). In many cases a more accurate definition of spectral indices makes doubtful the identification of a source as a SNR.

3. Results and discussion

Table 1 shows clearly that the main paramet many SNRs are corrected or obtained for the time. The total distribution of spectral indices i portant for statistical studies or classification (f ample, Glushak, 1991). It has an important affe the proposed dependences as to $\Sigma - D$ (surface b ness – diameter) and $N - D$ (number of sources $S > S_o$– diameter), which are used for evolutic models of SNRs. Further we consider some SN details. All the flux points accessible to the a were used to obtain spectra of the SNRs. Analy reliability of these measurements was made.

G0.0+0.0 This shell SNR Sgr A East is detect the Galactic Center, but special discussion is ne

G0.9+0.1 The source consists of compact an tended shells with different spectral indices (-0.1 and $\alpha_s = -0.6$) (hereafter $S \sim \nu^\alpha$). In ou servations we could measure only the total flux.

G1.4–0.1 This SNR was detected by Gray (19 Nearby bright Sgr A West complicates detecti this source at low frequencies. We could detect source only at 3.9 cm. The measurement deter a flat spectrum.

G1.9+0.3 The compact shell SNR was not reso in our observations, but the total flux densities measured with a high accuracy.

G2.4+1.4 The source was excluded by Green the new list of SNRs because it is a thermal optically visible around the early type star. But early observations showed it to have the non–the spectrum. They seem to suffer from confusion the Galactic center emission at the low frequency MHz. The last optical studies (Dopita et al., 199 allowed one to conclude that the shell was forme the star WR 102, blowing up cavity by the st wind.

G3.7–0.2 and G3.8+0.3 These are exte sources from the MOST survey at 843 MHz (1994b). They were determined as new SNRs bec of a shell morphology and non–thermal spectrum we could not detect these sources because of a complex background and environment.

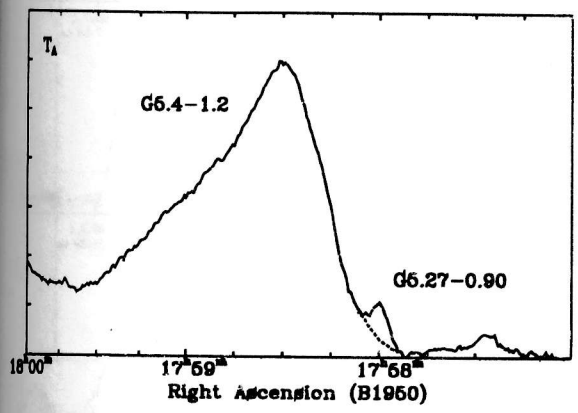

Figure 1: *SNR G5.4–1.2 at 3.9 GHz. The compact source G5.27–0.9 is on the western edge of the large SNR.*

G4.5–3.5 This source was identified as a SNR in the Effelsberg survey (Reich et al., 1990b). Our observations in the ZG–survey have shown that the spectrum is steep, coinciding with low frequency measurements (Kovalenko et al., 1994b).

G4.5+6.8 The well–known historical SN AD1604 shows now a clear shell structure without bright details. The obtained flux points are in agreement with the earlier measurements.

G5.4–1.2 This is a famous "duck–like" shell SNR, which has a compact source with the pulsar PSR 1758-24 in the "neck" (see Caswell et al., 1987; Manchester et al., 1991; Frail and Kulkarni, 1991). Fig.1 shows the linear brightness distribution of the SNR at Dec(1950) $= -24°51'30''$ at 7.6 cm wavelength. The neighbouring bright thermal complex M8 did not allow evaluation of total flux densities of the SNR. But for part of the source a flat spectrum is defined.

The main and remarkable feature of the compact source G5.27−0.90 consists in inverse spectrum with the distinguished in the synchrotron radiation theory spectral index $\alpha = +0.33$ (Fig.2). If a spectrum of relativistic electrons is cut off at low energy E_L, or in total they have the same energy E_L, then at a frequency lower than

$$\nu[GHz] = 16.1 \cdot H[10^{-3}Gs] \cdot E_L^2[GeV] \sin\theta$$

the spectral index of the optically thin source will be equal to $\alpha = 1/3$. The equipartitional magnetic field is estimated to be $10^{-4} - 5 \cdot 10^{-3}$Gs. The radio luminosity is about 10^{32} erg/s. It is most intriguing that the pulsar is in the bright tip of the compact source.

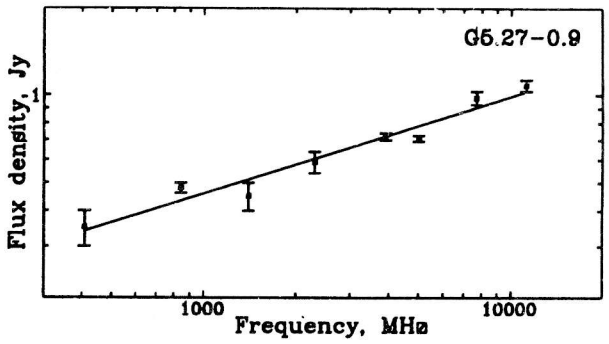

Figure 2: *Spectrum of G5.27–0.9. Spectrum with* $\alpha = +0.33$ *(straight line) fits the data points well.*

Simple model speculation implies that a pulsar, born in a SN explosion (now it is a big SNR) has received a great velocity and overtakes now an expanded shell, then it reaccelerates the electron of low energies in the bow shock, forming a compact source. But in a strong, up to $\approx 10^{-2}$ Gs, magnetic field, synchrotron losses are very high and the characteristic time of emission is equal to dozens of years. Therefore 50−100 years later the mono–energetic spectrum of electrons is formed in a region of energy, where the process of acceleration and losses went on the same time scale.

One of the probable reasons of mono–energetic spectrum formation is the mechanism of reacceleration of electrons in the region with magnetic reconnection, as proposed for Galactic Center Arc by Lerch and Reich (1992). In general, the model assumes that the powering of thermal electrons occurs in reconnection of magnetic lines of strength, where the induced electric fields accelerate the electrons up to relativistic energies. Probably in the source G5.27−0.90 the

Table 2: *Flux density measurements of the G5.27–0.90*

Frequency MHz	Flux mJy	Error mJy	References
408	350	50	1
843	476	20	1
1400	475	25	1
2300	580	50	2
3900	720	20	2
5000	717	15	1
7000	980	50	2
11200	1080	50	2

References:
(1) - Caswell et al.,1987
(2) - present paper

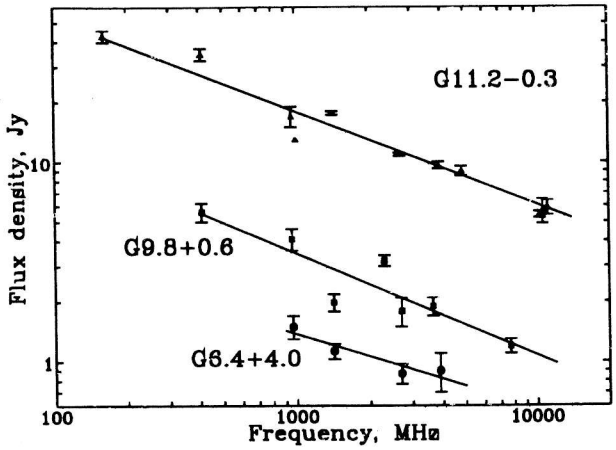

Figure 3: *Spectra of G6.4+4.0, G9.8+0.6 and G11.2−0.3.*

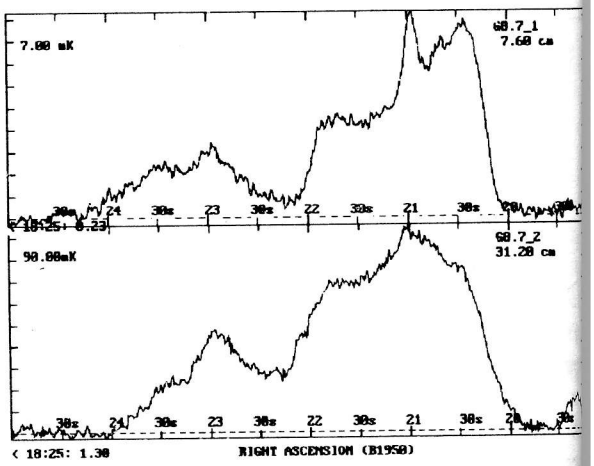

Figure 4: *The SNR G8.7−5.0 with the central comp source at two wavelengths.*

strong magnetic fields from the pulsar and the SNR shell have opposite orientations. The source is most likely to be powered by the fast short-period pulsar PSR 1758-24 (P = 125 ms).

G5.2−2.6 This source was also identified as a shell SNR in the Effelsberg survey (Reich et al., 1990b) and was included in the catalog of SNRs by Green (1995). But the flux density of this shell source is lower at 960 MHz than at 3900 MHz. This source was detected at 102 MHz (Kovalenko et al., 1994b).

G5.9+3.1 This new shell SNR was detected in the Effelsberg survey at 2.7 GHz (Reich et al., 1988). Our observations made the spectrum more accurate. It is fairly flat ($\alpha > -0.4$) which indicates a possible composite nature of the source, including the features of both shell and plerionic SNRs.

G6.1+1.2 This weak source was detected in the Effelsberg survey at 2.7 GHz (Reich et al., 1990b). Our observations have shown a steeper spectrum.

G6.1−0.1 This is a bright SNR W28 with the detected OH masers (Frail et al., 1994). The SNR was observed in the ZG-survey. Our flux points are consistent with the former spectrum.

G6.4+4.0 A new very faint shell SNR, with maximum brightness at its edges at 960 and 3900 MHz. The non-thermal spectrum is confirmed, as it is shown in Fig.3.

G7.7+3.7 For this SNR, detected in the Parkes observations at centimeter wavelengths, a clearly non-thermal spectrum has been obtained. Our observations allowed us to indicate a shell morphology.

G8.7−5.0 This is a SNR, detected in the Effe berg survey (Reich et al., 1988). It is located at t boundary of the ZG-survey (Trushkin, 1996). In Fi the distribution of brightness at two frequencies Dec(B1950)= $-23°50'$ is shown. The size of the V component is coincident with the sizes, derived by R ich et al. (1990b). The E-component seems to be a non-thermal. It is identified with the source MSH1 209 (31 Jy at 80 MHz). This interesting non-therm compact (< 1′) source 1820-239 is near the cen of the SNR. In Fig.5 its spectrum is shown. We us flux points from the Texas Preliminary, Molonglo a PMN surveys at 365, 408 and 4850 MHz, respectiv (database CATS; Verkhodanov, Trushkin, 1994). T spectral index is equal to $\alpha = -0.4$. This source see to be a variable source because during four mon the flux density at 3.9 GHz decreased from 300 to mJy. It seems to be analogous to SS433 in the S W50 (see below). The additional mapping obser tions with a high resolution are urgently needed.

G8.7−0.1 The complex W30 is identified non-thermal in the RATAN-600 observations Gosachinskij (1985). The summary spectrum is obtained in the range from 57 to 3900 MHz.

G9.8+0.6 Our measurements at 960, 2300, 3 3900 MHz supplemented the spectrum of this s source (Trushkin, 1989a). The spectrum is show Fig.2.

G10.0−0.3 This source is in a fairly confused reg of bright HII regions. Its morphology is not typi it has no plerion or shell structure. Our early observations with the "Southern sector+flat reflect antenna could not resolve the SNR. Now it is cl that G10.0−0.3 is confused with the bright HII

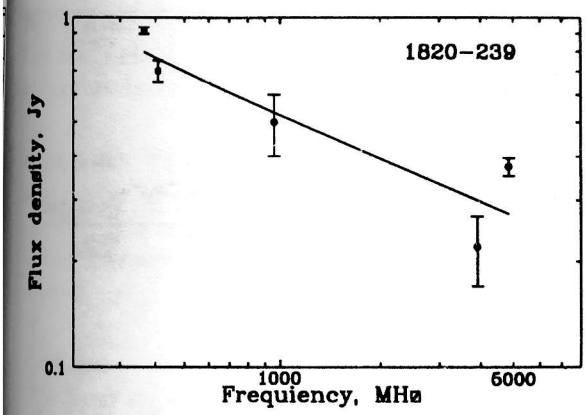

Figure 5: *Spectrum of the compact source 1820−239 being in the SNR G8.7−5.0.*

gion of G10.3−0.1 in the observations at low frequencies. New measurements with the Northern sector of the RATAN-600 allowed us to detect the source. It showed usual value of spectral index, $\alpha = -0.64$, typical for shell SNRs. At high frequencies, 7.7 and 11 GHz, the shell morphology is evident. Now this source is identified with the soft gamma-ray repeater SGR1806−20 (Kulkarni and Frail, 1993; Kulkarni et al., 1994). The high-frequency flux points are in good agreement with the VLA spectrum and there is no high-frequency turnover in this spectrum. It is interesting that the shell-like source, G9.7−0.1, visible on the VLA map of this region at 330 MHz (Kulkarni and Frail, 1993) seems to be an unknown SNR, because its spectrum is non-thermal, $\alpha = -0.60$.

G11.1−1.1 A new SNR detected by Trushkin (1986, 1989a) among the extended sources of the Effelsberg survey. It has not yet been included in the catalog of SNRs by Green (1995). Our and IRAS data show that the ratio IR/Radio< 100 differs from one for HII regions. Prominent H109α radiation in the direction of the source remains an unresolved problem of identification. The spectrum of this suspected SNR is shown in Fig.6.

G11.2−0.3 A clearly shell SNR with an edge-brightened radio emission. Earlier Downes (1984) considered its possible association with historical SN AD386, however from a comparison with other historical SNRs she concluded it to be a younger SNR with an age of 300−500 years. The spectrum is shown in Fig.2.

G11.4−0.1 Probably only a part of the ring shell remained, but the source is well detected against the local Galactic background.

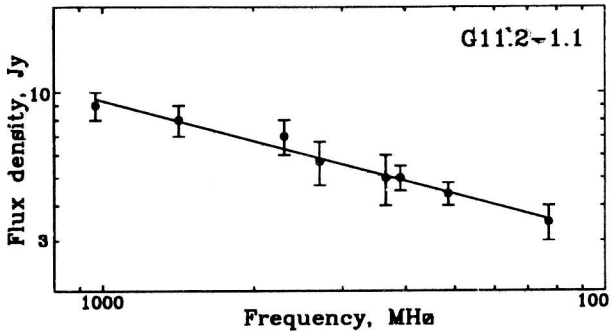

Figure 6: *Spectrum of G11.1−1.2. Straight line of fitting has the index* $\alpha = -0.45$

G12.0−0.1 The identification with a SNR (Clark et al., 1975) seems incorrect. The RATAN-600 observations at 3.9 and 11 GHz show two well-resolved sources: W-component is obviously an HII region ($\alpha = -0.1$) and the weak E-component with a steeper spectrum ($\alpha = -1.0$) is probably of extragalactic origin.

G13.5+0.2 The spectrum of this SNR is flatter ($\alpha = -0.9$), if using three additional flux points with the ones from the work of Helfand et al. (1989), but it is too steep for a typical SNR.

G15.1−1.6 This is a shell SNR near the Omega nebula complex. The change of the spectral index across the source is obvious because its size at 3.9 GHz is larger than that at 0.96 GHz. Thus, the spectrum is flatter at the edges of the SNR.

G15.9+0.2 This is a compact SNR, detected at the Australian radio telescopes (Clark et al., 1975). The shell morphology is well detected at 11 GHz, while the spectral index seems to change across the SNR and is steeper in the eastern part, as follows from the data at this frequency, 11 GHz.

G16.7+0.1 This is a new composite SNR with a compact center feature (Helfand el al., 1989) and flat spectrum, while our flux estimate is higher. Excluding clearly erroneous flux points the realistic spectral index, $\alpha = -0.4 \pm 0.1$, and the data at 11 GHz were used for the first time.

G16.8−1.1 This polarized source from the Effelsberg survey (Reich et al., 1986) is located at the boundary of the ZG-survey in the complex region. The measured flux density of this SNR at 0.96 GHz suggests a steep spectrum.

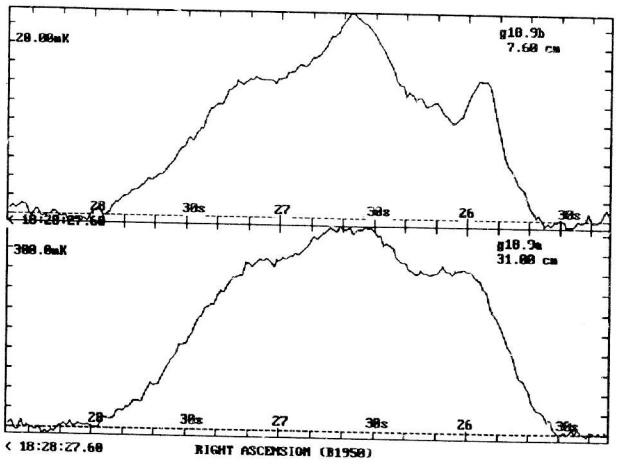

Figure 7: *The SNR G18.9–1.1 at two wavelengths.*

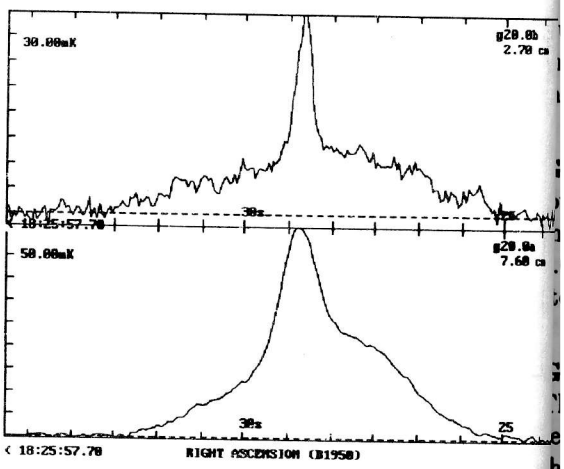

Figure 8: *The SNR G20.0–0.2 at two wavelengths. A compact HII region is projected onto the SNR.*

G17.4–2.3 and G17.8–2.6 These sources from the Effelsberg survey were observed in the ZG–survey (Trushkin, 1996). The former has arc–like morphology and was well detected at three wavelengths. The latter has a clear shell morphology. The nearby point source 1831–146 has a flat spectrum.

G18.8–0.3 The observations were carried out with the Southern sector of the RATAN–600. The flux densities were measured at 960, 2300 and 3650 MHz (Trushkin, 1989). The region of G18.8–0.3 was observed in the ZG–survey.

G18.9–1.1 This is one of the new SNRs, detected in the Effelsberg survey. The unusual structure with S–like feature drew attention at once (Furst et al., 1989). This detail has a flat spectrum (we obtained $\alpha = -0.20 \pm 0.05$), but no compact source in the center was identified on the radio maps, as it has been shown by Frail and Moffett (1992). This source belongs to the composite class of SNRs: a common shell is powered by a central source. The spectrum is measured in the range from 57 to 10000 MHz. The detail at the west edge of the SNR has $\alpha = -0.6 \pm 0.1$. In Fig.7 the linear brightness distribution at the 7.6 and 31 cm wavelengths is shown.

G20.0–0.2 Earlier this source was excluded from SNR catalog because of the flat spectrum. But the recognition of plerions with the flat spectra among SNRs makes one to return to observations (Becker and Helfand, 1989). The VLA map of this plerion shows an almost complete ring shell of edge–brightened structure. The spectral index is equal to $\alpha = -0.04$. The compact HII region projected onto SNR was identified with an OH–source. Its flat spectrum is typical of optically thin thermal radiation with a mean flux close to 1 Jy. The reliability of SNR identification is supported by the absence of recombination line H109α radiation in the direction of source. In Fig.8 the linear distribution of bright at the 7.6 and 31 cm wavelengths is shown.

G21.5–0.9 This is one of real plerions. This so was detected in the X–rays by space observa "Einstein". Recently Furst et al. (1988) have posed a model that assumes the diffuse central c ponent and complex axially symmetric structu magnetic field extending in the SNR, whereas and Moffett (1992) have not detected a compact source in it. A high–frequency turnover was dete by Salter et al. (1989).

G21.8–0.6 The shell SNR Kes 69 was observed the "Southern sector+flat reflector" at three w lengths. It showed unexpectedly high linear pola tion (up to 30 %).

G22.7–0.2 This shell SNR was confused with SNR G23.3–0.3. The ambiguous choice of bas did not allow us to determine the total flux densi The region at RA(B1950): $18^h29^m30^s - 18^h31^m$ Dec(B1950) $=-9°15'$ has a flat spectrum.

G23.6+0.3 This is a lucky case of reliable detec of a source in the observation with a fan beam pat in spite of nearby bright thermal sources. The s trum is steeper than it was earlier. The size is la by 30 %. Possibly it belongs to the class of compo SNRs.

G24.7+0.6 This SNR was detected in the Effelsb survey by Reich et al. (1984). We could detect only central part (RA(1950): $18^h30^m40^s - 18^h32^m00^s$.) in this region there was detected linear polarizati

But the spectrum of this region is flat. HII region to the south of the SNR has a flat spectrum with the mean flux density 3.0 ± 0.5Jy.

G24.7−0.6 The spectrum is well fitted by a power low, but the earlier measurements were confused with the flux of the nearby optically thin HII region (S_m = 1.0 Jy) and now we have found that the spectrum is steeper.

G27.4+0.0 This is an edge–brightened shell SNR. The X-ray compact source has been detected in the center, and its luminosity is equal to one fourth of the total L_X. But at radio waves this source has not been detected (Criss et al., 1985).

G27.8+0.6 It is a center–brightened large SNR detected in the early Effelsberg survey (Reich et al., 1984). Our three additional flux points define the spectrum as having $\alpha = -0.55$.

G29.7−0.3 This SNR Kes 75 is well detected at 11 GHz. It has a clear shell structure. We could not detect the compact source in the center, visible on the VLA map at 1.4 GHz (Becker et al., 1983). This SNR was detected in the X–ray range and is possibly associated with the X–ray pulsar GS 1843−24 (P=94.8 s).

G30.7+1.0 This is a SNR from the Effelsberg Galactic survey (Reich et al., 1986) at 2.7 GHz. The weak compact source is well detected at short wavelengths and has a flat spectrum (S_ν = 170 mJy).

G30.7−2.0 This is a SNR from the Effelsberg Galactic survey (Reich et al., 1988, 1990b) at 2.7 GHz. The weak compact source 1841−015 is well detected at 960 and 3900 MHz. It has a steep spectrum, but there is no clear shell morphology.

G31.9+0.0 The incomplete shell of the SNR indicates different conditions of expansion of SNR in ISM, whereas the E–edge is 8–10 times weaker than the W–edge, which is closer to the plane of the Galaxy. This SNR is larger than it was estimated earlier, and in the eastern direction the radiation extended up to 10′, while at a distance of 7.5′ the level of radiation is higher than 10 noise rms. The detailed studies of this SNR were carried out by Moffett and Reynolds (1994).

G32.8−0.1 This source is well detected at 3.9 GHz against the complex Galactic background. But the spectrum is flat. There is a discrepancy with the data at 330 MHz (Kassim, 1992).

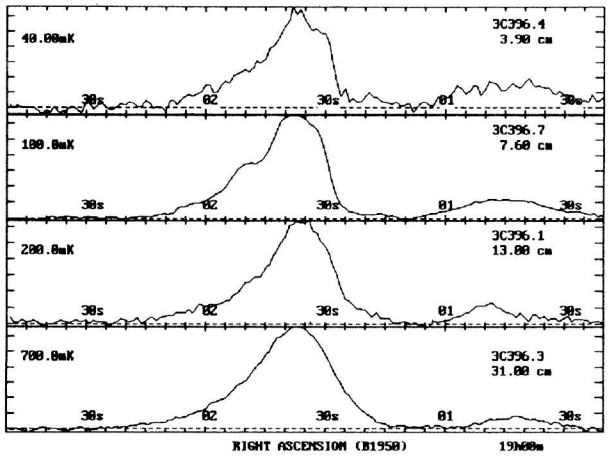

Figure 9: *The SNR G39.2−0.3 (3C396) at four wavelengths.*

G33.6+0.1 It is a bright moon–like crescent SNR. Its spectrum is obtained in the range from 30 to 11000 MHz. In the shell the variable compact flat spectrum source 1849+005 is detected.

G34.7−0.4 This is the well–known bright shell SNR W44 with a fairly flat spectrum. Our flux points are in good agreement with the former spectrum.

G36.6+2.6 This is a very weak source detected at three frequencies. The spectrum is flat ($\alpha = -0.18$) rather than steep as in earlier measurements of Reich et al. (1990b).

G36.6−0.7 This source seems to be a false identification of the extended non–thermal source with SNR. Its elongated structure and very steep spectrum ($\alpha = -1.0$) strongly resemble an extragalactic source.

G39.2−0.3 It is the well–known SNR 3396, formerly considered as plerion. As in G31.9−0.3 its western and eastern edges differ ten times and form the complete shell. The remarkable "tail" of emission was found at the eastern edge of the SNR. Strong linear polarization and X–ray radiation were detected. This source seems to belong to the class of composite SNRs. In the eastern direction the source extends far away beyond the source boundaries detected by Becker and Helfand (1987) as shown in Fig.9, but it is the same as in the VLA maps which was received by Anderson and Rudnick (1993) at 1.45 and 4.9 GHz. Our old evaluations of the flux suffer from incorrect low baselines, but new data reduction of the same observations gave slightly smaller values of the flux densities. The contribution of nearby sources to the total fluxes is very small. Probably the contribution

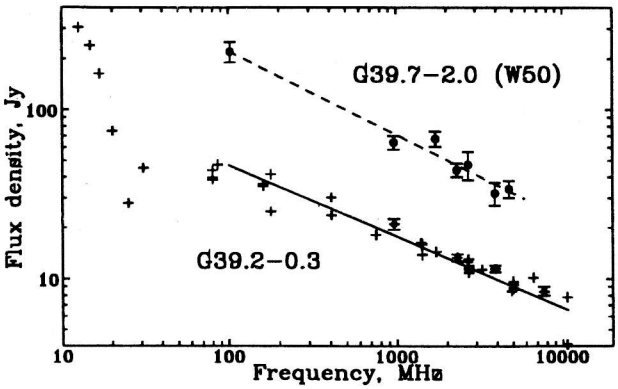

Figure 10: *Spectra of 3C396 and W50. In the spectrum obtained by Patnaik et al. (1990) (straight line and crosses) the RATAN points were included (black squares).*

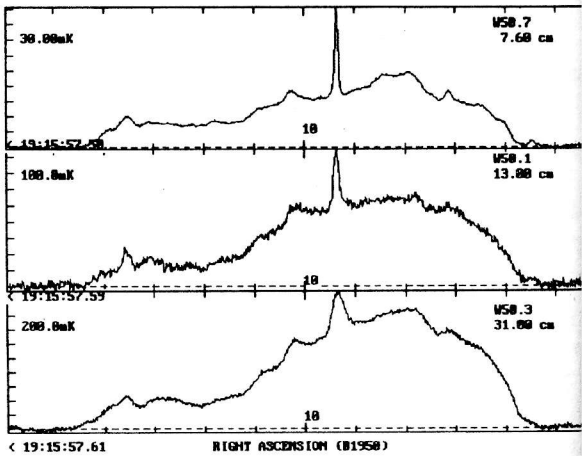

Figure 11: *The SNR G39.7−2.03 W50 at three wa lengths.*

of the "tail" to the total flux of the SNR is noticeable.

The unusual increase in the radio spectrum at low frequencies (Fig.10) may be interpreted as a contribution of an undetected pulsar, while Patnaik et al. (1990) considered this to be a result of unusually high depth value $\tau = 3.3$ at 12.6 MHz. Possibly at low frequencies the radiation from the nearby pulsar PSR 1900+05 could get into the beam pattern.

G39.7−2.0 In this well-known SNR W50 there is a peculiar close binary system SS433, the emission star, variable radio and X-ray source. The clear shell morphology is disturbed by jets from SS433. The distributions of brightness at three frequencies are given in Fig.11. The spectrum of W50 (Fig.10) was obtained using only the flux points considering the large size, 120′. in RA direction (Downes et al., 1981; Kovalenko et al., 1994b). It is well fitted by a power law with $\alpha = -0.50$.

G40.5−0.5 This shell SNR has no peculiarities at radio wavelengths. The obtained spectrum is more flat, than it was determined earlier.

G41.1−0.3 The spectrum obtained was unexpectedly very steep. The former measurements included the contribution of the thermal source G41.1−0.3W with the flux S ($\nu \geq 4$ GHz) = 4-5 Jy. Our observations distinguished two sources more sure. The SNR has a clear shell structure as shown in X-ray data by Becker et al. (1985).

G42.8+0.6 This is a weak shell SNR with a steep spectrum, detected in the Effelsberg survey.

G43.3−0.2 This is a bright shell SNR W49B n the powerful HII region W49A, which we used measurements as a calibration source.

G43.9+1.6 This SNR attracted attention becau it is likely associated with the soft γ-ray repeat 1900+14. However Vasisht et al. (1994) did not veal any obvious plerionic features in the VLA servations at 327 MHz. We could estimate the sp trum of two prominent features of the proposed SN The source G44.0+1.3 has a flat spectrum similar that of an optically thin HII region. The feature G44.2+1.8 has a spectrum with $\alpha = -1.0$ absolut unlike that of the SNR. The VLA map at 327 MHz dicates it has two different components. Thus, the f ture seems to be a background extragalactic sour while it is within the error box of the soft γ-ray peater 1900+14.

G45.7−0.4 This is a new low-brightness SNR tected in the Effelsberg survey. Our value of the fl at 31 cm wavelength is three times higher than t former estimates in this wavelength range. Thus, t spectrum is steeper.

G46.8−0.3 This bright SNR HC30 shows a sh structure. In the earlier observations the flux val from the nearby sources were included.

G49.2−0.7 This is a compound source W51. T extended SNR is observed against the foreground bright HII regions. In the recent paper Copetti a Schmidt (1991) discussed the features of the sour in this complex at 151 MHz. It was confirmed th W51 is a shell SNR so far as no recombination li radiation was detected but the X-ray radiation present in it. The spectrum was defined with α

-0.31 for the whole complex, the flatter one because of the great contribution of optically thin HII regions. The spectrum of the SNR without HII region is determined with the spectral index $\alpha = -0.65 \pm 0.05$.

G53.6–2.2 This SNR 3C400.2 is well detected against the weak Galactic background. The spectrum is well fitted by a power law. This SNR has a clear shell radio structure, and X–ray emission with the central peak is detected, as shown by Long et al. (1991). The latter can be explained by models, suggesting evaporation of cloudlets of interstellar medium in the shock passing through them. It results in increasing the density of the hot gas within SNR.

G54.1+0.3 This is a compact plerion SNR unresolved in our observations. The flat spectrum is confirmed. The SNR is in the center of the complex HC40.

G54.4–0.3 This SNR HC40E has a steep spectrum, while HC40W is a thermal source, as suggested by Caswell (1985). Our observations confirmed the non–thermal origin of the eastern part of the source.

G55.7+3.4 This faint source was detected as a SNR by Goss el al. (1977) in WSRT observations and Kovalenko et al. (1994b) at 83 MHz with the BSA telescope. The spectrum is well fitted by a power law with $\alpha = -0.53$.

G57.2+0.8 Some years ago this source was associated with the 1.5 ms pulsar 1930+22. But the distances for them differ very much, thus the SNR and the pulsar seem to have no connection. We obtained a more accurate spectrum using three new flux points.

G59.5+0.1 It is one of the new unreliably defined SNRs, detected by Taylor et al. (1992) near the nebula S83. The spectrum is well fitted by a power low with $\alpha = -0.57$. The spectrum is shown in Fig.12.

G59.8+1.2 This is one of the new unreliably defined SNRs. The spectrum indicates a really critical value $\alpha = -0.32$. It shows the presence of linear polarization (Junkes et al., 1990.) The spectrum is shown in Fig.12.

G65.7+1.2, G65.1+0.6 The two SNRs are in the same region. Seven cross–sections in declination are needed to observe this large region. There are some compact sources in the area of the SNRs. The spectrum of the smaller SNR G65.7+1.2 was obtained. In the second SNR the spectral index does not change in RA.

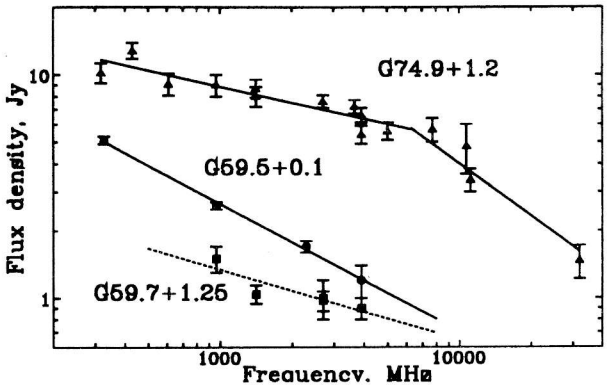

Figure 12: *Spectra of G59.5+0.1, G59.8+1.2 and G74.9+1.2. A spectrum of $\alpha = -0.32$ (dashed line) fits the data points well. The CTB87 is defined by a dual–power low spectrum (straight line).*

G67.7+1.8 Our measurements indicate a much steeper spectrum of this source. Excluding the flux point at 327 MHz the spectrum is well fitted by a power law with the index $\alpha = -1.0$. It is typical rather of radio galaxies than of SNRs.

G68.6–1.2 This very weak source was detected only at 3.9 GHz. It has two brighter details, and no clear shell morphology.

G69.7+1.0 This weak SNR was detected in the Effelsberg survey (Reich et al., 1988; 1990b). Our values of the flux are much higher than the earlier ones, while the non–thermal spectrum is confirmed.

G69.0+2.7 The SNR CTB80 is a quite unordinary SNR. Its large scale structure was indicated with three ridges of radio emission, extended up to 30′ from the center, where the 10′ plateau and the compact flat spectrum core at its western edge are clearly detected in our observations. The core identified with filamentary optical nebulosity is slightly elongated, having a size of 40″. At the western edge of the core the 40 ms pulsar PSR 1951+32 was detected.

In Fig.13 the linear distribution of brightness is shown across the plateau and core at the declination of the pulsar. In Fig.14 their spectra are shown. The spectral index of the plateau is $\alpha = -0.52 \pm 0.05$. The spectrum of the core was obtained in the range from 960 to 14400 MHz and it was flat, but unexpectedly with the mean flux close to 1 Jy, different from the early estimates by nearly 0.5 Jy (Angerhofer et al., 1981; Sofue et al., 1983). But if the core flux value, 300 mJy at 84 GHz by Salter et al. (1989), was used, a turnover at high frequencies seems to be probable in the core spectrum. No confusion occurs in the region of CTB80. Firstly, we suggested variability of

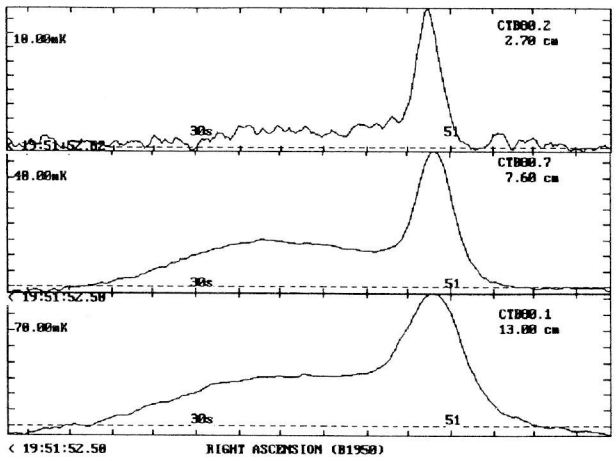

Figure 13: *The central part of the plateau of CTB80 at three wavelengths at declination of the core.*

the core flux on a scale of a few years, but the four runs of observations in 1988, 1989, 1991 and 1996 did not show essential differences in the spectrum. Probably at high frequencies the spectrum has the turnover at 8–10 GHz as the spectrum of the epoch 1996 did (1250, 1150, 1040, 980, 750 mJy at 0.96, 2.3, 3.9, 7.7 and 11.2 GHz, respectively). Possibly the earlier points suffer from the difficulty of separating the core from the plateau. Our flux points have the errors less than a few percent. It should be noted that in the optical core of CTB80 Strom (1988) observed wisp–like phenomena as in the Crab nebula. And during 6 years the bulk motion with a velocity of $0.1 \cdot c$ could result in changes in the total radio flux of the core. Obviously the short pulsar phenomena are possible in the magnetosphere on such time scales.

G73.9+0.9 The spectrum of this SNR identified in the Effelsberg survey is flatter. Three compact sources found at 4850 MHz were detected in our observations. Recently Pineault and Chastenay (1990) have obtained radio maps at 408 and 1420 MHz with the interferometer of DRAO. They concluded that the SNR is a plerion rather than a shell, as confirmed by our measurements of the spectra.

G74.9+1.2 CTB87 is one of good examples of plerions. An important feature of its spectrum is a break in the region $\nu_b = 6500$ MHz ($\nu < \nu_b$, $\alpha = -0.24$; $\nu > \nu_b$, $\alpha = -0.78$) (Fig.12). The break is easily explained by synchrotron losses without additional sources of energy. Then the magnetic field in the plerion would be of the order of $5 \cdot 10^{-3}$ Gs. On the other hand the SNR could have two distributions of electrons with different spectra of energy. One is from the invisible pulsar, the other generated by the shock wave of the expanding SNR.

G78.2+2.1 This is a very large and bright SN DR4 in the Cygnus X region. The measured poi are consistent with the former spectrum with α -0.53. The bright feature to the south from the ce ter, RA(1950): $20^h20^m52^s$, Dec(1950)=40°03′), ha steeper spectral index, $\alpha = -0.59$.

G83.0−0.2 This source was detected as a SNR Taylor et al. (1992), but it is absent in recent Gree catalog of SNRs (1995). Our measurements at th frequencies suggest a flat spectrum.

G84.2−0.8 This is a well defined SNR (Matthews al., 1980). Our flux points supplement the spectr with the new value $\alpha = -0.62$.

G84.9+0.5 This source was also detected by Tay et al. (1992) at 327 and 4850 MHz. It is confused wi the arc–like feature G84.6+0.2 at 0.96 and 2.3 GH The total size of the source is 10′. But the flux 11 GHz is much higher than the flux density at 4 GHz. Thus the spectrum only with our flux point fitted by a power law with $\alpha = -0.65$.

G85.2−1.2 Taylor et al. (1992) defined this sou as a SNR, but it is not included in Green's catalog SNRs (1995). Only from our measurements at th frequencies a flat spectrum was obtained.

G327.6+14.6 This is the remnant of the SN AD1006, a typical shell SNR (Fig.11). Its symmet

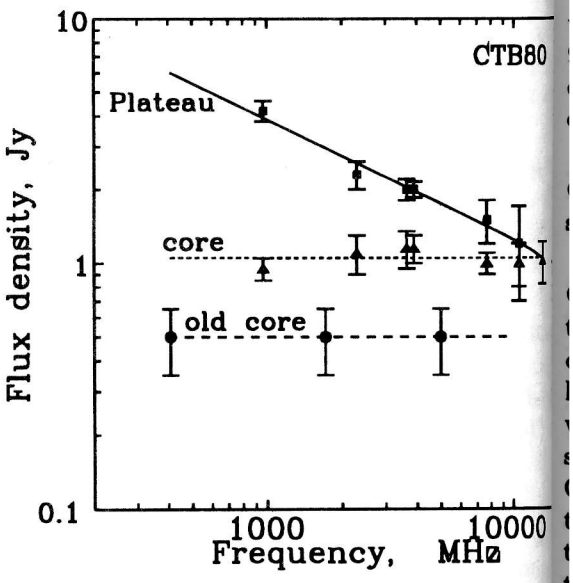

Figure 14: *Spectra of the features of CTB80. The sp tra of the "core" (dashed lines) fitted for earlier tected — "old" and current points. All available poi were used.*

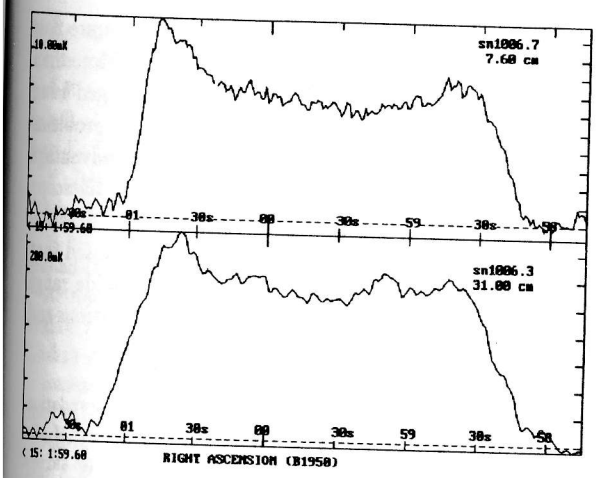

Figure 15: *The remnant of the historical SN AD1006 at two wavelengths.*

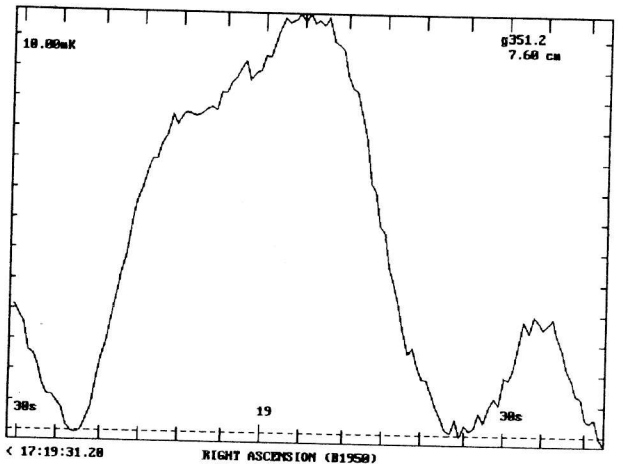

Figure 16: *The SNR G351.2+0.1 at 3.9 GHz.*

form allowed a model with a quasi–isotropic magnetic field for determination of geometric parameters to be used. This is the case, when the integral synchrotron emissivity depends only on the radius and depth of the shell. If the radial magnetic field is taken into account, then the different pitch–angles must be considered. The integrals are converted to special functions and calculated numerically. Then a comparison of the model and observed distributions of brightness or radial profile of SNRs gives a diameter of 30′ and a depth of 5′ for the SN AD1006. These parameters are consistent with the X–rays data for the shell (Trushkin, 1989b).

G344.7−0.1 A larger number of flux measurements were used for the spectra of this SNR. The data at 960 and 3900 MHz were added. Dubner et al. (1993) obtained a VLA map at 1.47 GHz. This SNR was observed in the ZG–survey (Trushkin, 1995).

G346.6−0.2 We could determine the size and the spectrum of this SNR.

G348.5+0.1, G348.5−0.0, G348.7+0.3 The first two bright SNRs, CTB37A and CTB37B, are indicated at same kinematic distance, 10.2 kpc. The arc–like detail in the eastern part of 37 was identified with the third SNR G348.5−0.0 in this region (Kassim et al., 1991). It is well detected from the nearby CTB37A in our observations. For G348.5−0.0 we obtained $\alpha = -0.55$, while the neighbouring SNR has the spectral index $\alpha = -0.46$, steeper than that obtained previously.

G349.7+0.2 This SNR is the third in brightness after Cas A and Crab Nebula. It is a SNR from the composite class of SNRs. The spectrum was followed from 80 to 11100 MHz. The bright detail at the center was not resolved in the VLA observations at the 6 cm wavelength (beam 10″). High resolution mapping is needed for this very interesting compact source.

G350.0−1.8 This SNR has a clear shell form. But the flux density at 1 GHz is two times lower than the earlier value (Green, 1988). The summary spectrum has the same spectral index $\alpha = -0.5$.

G350.1−0.3 This source was confused with the HII region to the south of this source in earlier measurements. Our observations indicate $\alpha = -0.69$, but if all the available flux points were used, the spectrum would steeper. Thus probably it is an extragalactic source rather than a SNR.

G351.2+0.1 This shell SNR has a compact source at the center which has a flat or inverse spectrum and the mean flux $S_m = 12 \pm 3$ mJy (Fig.12). This SNR belongs probably to the composite class of SNRs. The bright thermal gas complex is near the SNR.

G352.7−0.1 In our observations radiation from the bright thermal source is confused with radiation of the SNR, but we could exclude its contribution. The spectrum was followed from 408 up to 11100 MHz.

G355.9−2.5 The obtained distributions of brightness across this shell SNR are in good agreement with the MOST map at 843 MHz (Caswell et al., 1984).

G357.7−0.1 This is one of the brightest and unusual SNR MSH 17−39. Its intensity at opposite edges differs by a factor of 20 (Fig.13). Obviously the conditions of radio evolution and expansion of the SNR changed on Galactic scales of a few parsecs. The linear polarization was measured at 7.7 GHz. It has a

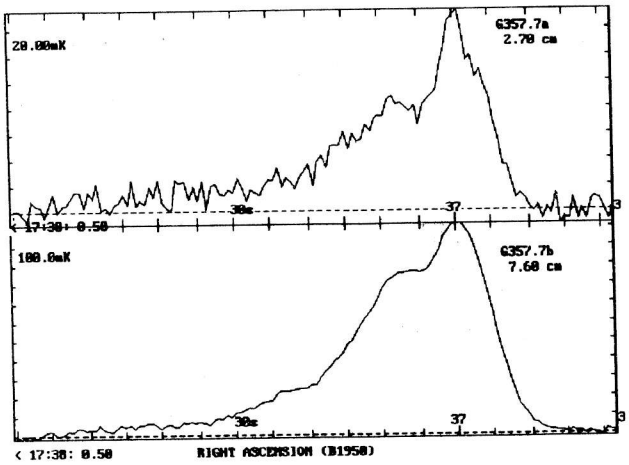

Figure 17: *The SNR G357.7−0.1 at two wavelenghts.*

maximum in the western part p = 10 % . Its position angle is changes in RA direction from $\chi = 35^o$ up to 70^o near the brightest part of the SNR. Convolution of the distribution of brightness at the 1.4 GHz wavelength obtained by Shaver at al. (1985) with VLA and the beam pattern of the RATAN–600 at the 7.6 cm wavelength allowed us to model our linear drift scans. It shows no steepening of spectra in the direction of weaker regions of the SNR as one might expect if the more distant regions are powered from more brighter ones. Thus "aging", possible on the scale of thousands of years of such electrons was not detected. Probably the difference of synchrotron luminosity in this region is associated with the conditions of shock propagation in the local ISM.

G357.7+0.3 This source remains an unconfirmed SNR, because the spectrum is close to thermal. A flux density at 960 MHz could not change if used other determination of the background. The source was detected in the Effelsberg Galactic survey at 2.7 GHz. A new MOST map at 843 MHz was obtained by Gray (1994).

G359.1−0.5 This source from the Effelsberg survey (Reich and Fusrt, 1984) shows a flat spectrum, although this region is very confused.

4. Conclusion

Results of observations of the SNRs during several years are presented. Measurements of integrated flux densities at least at two-four frequencies, using one radio telescope allowed us to refine the spectra of ≈ 90 out of 107 SNRs, visible with the RATAN-600 in the Galactic quadrants I and IV. The data are useful for obtaining spectra in a wide frequency range. The non–thermal spectra of 17 SNRs have been confirmed. But the spectra of 16 suspected shell SNRs are fl which is not typical of this shell SNR class. More th a dozen SNR spectral indices have been changed usi our new flux measurements. The statistical proble can be resolved with new data. It is the advanta of the RATAN–600 as a multi–frequency telesco that allowed reliable measurement of flux densiti even in the confused regions. It should be noted th high sensitivity, moderate resolution and wide ra of the frequencies are very useful in investigations a search of SNRs.

Acknowledgements. I thank the Russian Foundati of Fundamental Researches for partial support of t work, including the results of the RATAN Galactic surv (grant 93–02–17086). I thank Yu.N. Parijskij for conti uous interest in the work. I thank the colleagues, w took part in current software development, T. Sokolo V. Chernenkov, G. Mal'kova, O. Verkhodanov, I. Lichr and T. Plyaskina, and especially G. Zhekanis for g operation of antenna.

References

Aliakberov K.D., Mingaliev M.G., Naugolnaya M. Trushkin S.A., Sharipova L.M., Yusupova S.N.: 19 Astrofiz. Issled. (Isv. SAO), **19**, 60.

Anderson M.C., Rudnick L.: 1993, Astrophys. J., 4 514.

Angerhofer P.E., Strom R.G., Velusamy T., Kundu M. 1981, Astron. Astrophys., **94**, 313.

Arendt R.: 1989, Astrophys. J. Suppl. Ser., **70**, 181.

Baars J.W.M., Genzel R., Pauliny–Toth I.I.K., Witzel 1977, Astron. Astrophys., **61**, 99.

Becker R.H., Helfand D.J.: 1985, Astrophys. J., **297**,

Becker R.H., Helfand D.J.: 1987, Astron. J., **94**, 162

Becker R.H., Markert T., Donahue M.: 1985, Astroph J., **296**, 461.

van den Berhg S.: 1983, IAU Symp. No.101, Super remnants and their X–rays emission, eds.: Danzig and Gorenstein, 594.

Beichman C.A., Neugebauer G., Habing H.J., Clegg P Chester T.J.: 1988, NASA RP–1190, *Infrared As nomical Satellite (IRAS), Catalogs and Atlases*, 1, planatory Supplement.

Caswell J.L.: 1985, Astron. J., **90**, 1224.

Caswell J.L., Kesteven M.J., Komesaroff M.M., Ha R.F., Milne D.K., Stewart R.T., Wilson S.G.: Mon. Not. R. Astron. Soc., **225**, 329.

Clark D.H., Green A.J., Caswell J.L.: 1975, Aust. J. P Astrophys. Suppl., No. 37, 1.

Copetti M.V.F., Schmidt A.A.: 1991, Mon. Not. R. tron. Soc., **250**, 127.

Downes A.J.B.: 1984, Mon. Not. R. Astron. Soc., 855.

Downes A.J.B., Pauls T. Salter C.J.: 1981, Astron. As phys., **103**, 277.

Dopita M.A., Lozinskaya T.A., McGregor P.J., Rawl S.J.: 1989, Astrophys. J., **351**, 563.

Dopita M.A., Lozinskaya T.A.: 1990, Astrophys. J., 419.

Dubner G.M., Moffett D.A., Goss W.M., Windker P.F.: 1993, Astron. J., **105**, 2251.
Frail D.A., Kulkarni S.R.: 1991, Nature, **352**, 785.
Frail D. A., Moffett D.A.: 1993, Astrophys. J., **408**, 637.
Furst E., Hummel E., Reich W., Sofue Y., Sieber W., Reif K., Dettmar R.-J.: 1989, Astron. Astrophys., **209**, 361.
Handa T., Sofue Y., Nakai N., Hirabayashi H., Inoue M.A.: 1987, Publ. Astron. Soc. Japan., **39**, 709.
Helfand D., Velusamy T., Becker R.H., Lockman F.: 1989, Astrophys. J., **341**, 151.
Hughes V.A., MacLeod G.C.: 1989, Astron. J., **97**, 786.
Glushak A.P.: 1991, in: Proceed. XXV radioastronomical conference, Ashkhabad, ed.: Ylym. 71.
Goss W.M., Scharz U.J., Sidesh S.G., Weiler K.W.: 1977, Astron. Astrophys., **61**, 93.
Gray A.D.: 1994a, Mon. Not. R. Astron. Soc., **270**, 836.
Gray A.D.: 1994b, Mon. Not. R. Astron. Soc., **270**, 847.
Green D.A.: 1988, Astrophys. Space Sci., **148**, 3.
Green D.A.: 1991, Publ. Astr. Soc. Pacific, **103**, 209.
Green D.A.: 1995, A Catalogue of Galactic Supernova Remnants (*1995 July version*), MRAO, UK (available on the WWW at "http://www.phy.cam.ac.uk./www/research/ra/SNRs/snrs.intro.html").
Kassim N.E.: 1989, Astrophys. J. Suppl. Ser., **71**, 799.
Kassim N.E., Baum S.A., Weiler K.W.: 1991, Astrophys. J., **374**, 212.
Kassim N.E.: 1992, Astron. J., **103**, 943.
Kovalenko A.V. Pynzar' A.V., Udal'tsov V.A.: 1994a, Astron. Zh., **71**, 92.
Kovalenko A.V. Pynzar' A.V., Udal'tsov V.A.: 1994b, Astron. Zh., **71**, 110.
Kriss G.A., Becker R.H., Helfand D.J., Ganzales C.R.: 1985, Astrophys. J., **288**, 703.
Kulkarni S.R., Frail D.A.: 1993, Nature, **365**, 33.
Kulkarni S.R., Frail D.A., Kassim N.E., Murakami T., Vasisht G.: 1994, Nature, **368**, 129.
Lerch H., Reich W.: 1992, Astron. Astrophys., **264**, 493.
Long K.S., Blair P., White R., Matsui Y.: 1991, Astrophys. J., **373**, 567.
Manchester R.N., Kaspi V. M., Johnston S., Lyne A.G., D'Amico N.D.: 1991, Mon. Not. R. Astron. Soc., **253**, 7.
Matthews H.E., Shaver P.A.: 1980, Astron. Astrophys., **274**, 421.
Moffett D.A., Reynolds S.P.: 1994, Astrophys. J., **425**, 668.
Odegard N.: 1986, Astron. J., **92**, 1372.
Patnaik A.K., Huant G.C., Salter C.J., Shaver P.A., Velusamy T.: 1990, Astron. Astrophys., **232**, 467.
Pineault S., Chastenay P.: 1990, Mon. Not. R. Astron. Soc., **246**, 169.
Reich W., Furst E.: 1984, Astron. Astrophys. Suppl. Ser., **57**, 165.
Reich W., Furst E., Sofue Y.: 1984, Astron. Astrophys., **133**, L4.
Reich W., Furst E., Reich P., Sofue Y., Handa T.: 1986, Astron. Astrophys., **151**, 185.
Reich W., Furst E., Reich P., Junkes N.: 1988, in: Supernova remnants and the Interstellar Medium, *IAU Colloquim N101*, eds.: Roger R.S and Landecker T.L. (Cambridge University Press), 293.
Reich W., Reich P., Furst E.: 1990a, Astron. Astrophys. Suppl. Ser., **83**, 539.
Reich W., Furst E., Reich P., Reif K.: 1990b, Astron. Astrophys. Suppl. Ser., **85**, 633.
Salter C.J., Reynolds S.P., Hogg D.E., Payne J.M., Phodes P.J.: 1989, Astrophys. J., **338**, 171.
Seward F.:1990, Astrophys. J., **73**, 781.
Shaver P.A., Salter C.J., Patnaik A.R., van Gorkom J.H., Hunt G.C.: 1985, Nature, **313**, 113.
Sofue Y., Takahara F., Hirabayashi H., Inoue M., Nakoi N.: 1983, Publ. Astron. Soc. Japan, **35**, 437.
Strom R. G., Blair W.P.: 1985, Astron. Astrophys., **149**, 259.

Taylor A.R., Wallace B.J., Goss W.M.: 1992, Astron. J., **103**, 931.
Trushkin S.A.: 1986a, Astron. Circular, **1453**, 4.
Trushkin S.A.: 1986b, Pis'ma Astron. Zh., **12**, 198.
Trushkin S.A., Vitkovskij V.V., Nizhelskij N.A.: 1988, Astrofiz. Issled. (Izv. SAO), **25**, 84.
Trushkin S. A.: 1989a, Ph.D. Thesis. SAO RAS, Nizhnij Arkhyz.
Trushkin S.A.: 1989b, Prepr. SAO RAS, No. 32.
Trushkin S.A.: 1989, Prepr. SAO RAS, No. 38.
Trushkin S.A.: 1991a, Astrofiz. Issled. (Izv. SAO), **32**, 132.
Trushkin S.A.: 1991b, in: Proceed. III radioastronomical conference, Ashkhabad, ed.: Ylym, 70.
Trushkin S.A.: 1993a, in: Proceed. XXV radioastronomical conference, Pushchino, FIAN, 76.
Trushkin S.A., 1993b, in: Proceed. XXV radioastronomical conference, Pushchino, FIAN, 84.
Trushkin S.A.: 1994, Prepr. SAO RAS, No. 107.
Trushkin S.A.: 1996, Astron. Astrophys. Trans., (in press).
Verkhodanov O.V., Trushkin S. A.: 1994, Preprint SAO RAS, No. 106, 66.
Verkhodanov O.V., Vitkovskij V.V., Eruhimov B.L., Zhelenkova O.P., Likhvan O.P., Monosov M.L., Chernenkov V.N., Shergin V.S.: 1993, Prepr. SAO RAS, 91L, 18.
Vitkovskij V.V.: 1990, Ph.D. Thesis, SAO RAS, Nizhnij Arkhyz.
Whiteoak J.B.Z.: 1992, Astron. Astrophys., **262**, 251.
Whiteoak J.B.Z., Green A.: Astron. Astrophys. Suppl. Ser., 1996, in press.